Effect of two forms of feedback on the performance of the Rate Control Protocol (RCP)

Abuthahir[a,*], Nizar Malangadan[a], Gaurav Raina[a]

[a]*Department of Electrical Engineering, Indian Institute of Technology Madras, Chennai-600036, India*

Abstract

The Rate Control Protocol (RCP) uses explicit feedback from routers to control network congestion. RCP estimates it's fair rate from two forms of feedback: rate mismatch and queue size. An important design question that remains open in RCP is whether the presence of queue size feedback is helpful, given the presence of feedback from rate mismatch. The feedback from routers to end-systems is time delayed, and may introduce instabilities and complex non-linear dynamics. Delay dynamical systems are often modeled using delay differential equations to facilitate a mathematical analysis of their performance and dynamics. The RCP models with and without queue size feedback give rise to two distinct non-linear delay differential equations. Earlier work on this design question was based on methods of linear systems theory. For further progress it is quite natural to employ nonlinear techniques. In this study, we approach this design question using tools from control and bifurcation theory. The analytical results reveal that the removal of queue feedback could enhance both stability and convergence properties. Further, using Poincaré normal forms and center manifold theory, we investigate two nonlinear properties, namely, the type of Hopf bifurcation and the asymptotic stability of the bifurcating limit cycles. We show that the presence of queue feedback in the RCP can lead to a sub-critical Hopf bifurcation, which would give rise either to the onset of large amplitude limit cycles or to unstable limit cycles. Whereas, in the absence of queue feedback, the Hopf bifurcation is always super-critical and the bifurcating limit cycles are stable. The analysis is complemented with computations and some packet-level simulations as well. In terms of design, our study suggests that the presence of both forms of feedback may be detrimental to the performance of RCP.

Keywords: Congestion control, Rate control protocol, queue feedback, stability, convergence, Hopf bifurcation

*Corresponding author at: Department of Electrical Engineering, Indian Institute of Technology Madras, Chennai-600036, India.

Email addresses: ee12d207@ee.iitm.ac.in (Abuthahir), ee11s040@ee.iitm.ac.in (Nizar Malangadan), gaurav@ee.iitm.ac.in (Gaurav Raina)

1. Introduction

Most queuing systems routinely share information regarding waiting times, or queue lengths, with customers. Such information can certainly influence the behavior of customers. If such feedback is not instantaneous, but is time-delayed, it can have a significant impact on the underlying system dynamics; for example, see [1, 24, 25, 29]. The presence of feedback delays makes the system infinite-dimensional, and may pose numerous theoretical and practical challenges. In general, the stability of a closed-loop system is sensitive to feedback delays, which normally necessitates a detailed stability analysis. Local stability analysis retains only the linear component and ignores all higher order terms of the nonlinear system before addressing the issue of stability. However, the feedback delays of a nonlinear dynamical system may result in various complex dynamics like bifurcation, chaos, etc. So, it looks appealing to have an analytical methodology which may allow us to capture the impact of some nonlinear terms while performing a Taylor expansion of the nonlinear system about its equilibrium. Local bifurcation theory is one such methodology [11]. For example, see [5, 14, 18, 24] for some stability and bifurcation analysis of dynamical systems with feedback delays. Moreover, without an understanding of the dynamics of the system in the unstable regime, choosing an operating point close to the boundary of the stable region could be risky. A comprehensive understanding of local bifurcation phenomena may help yield insights into the behavior of the system in the unstable regime. This paper employs both linear systems theory and non-linear techniques to investigate how the feedback of queue size can impact the system behavior in the setting of congestion control protocols for the Internet. We consider protocols where end-systems use feedback, which is time-delayed, from routers to adjust their rates. There is a continued interest in analyzing the stability and dynamical properties of fluid models for Internet congestion control algorithms [10, 22, 26, 27, 34, 38]. In this paper, our focus will be on a well-known congestion control transport protocol called the Rate Control Protocol (RCP) [2, 6, 16, 17, 19].

Internet congestion control has been an active area of networking research for several decades [31]. The Transmission Control Protocol (TCP) is currently the most commonly used transport protocol, which handles congestion control in the Internet. The widespread use of high bandwidth-delay networks and wireless links create limitations on the performance of standard TCP. Currently, TCP uses packet loss and delay as signals of network congestion. But, delay and loss are damage to packets, and hence this implicit signaling mechanism affects the performance limits and system Quality of Service (QoS). This has led to the development of congestion control protocols that could employ explicit feedback. Some examples of explicit congestion control algorithms include the Rate Control Protocol (RCP) [2, 6, 16, 17, 19], eXplicit Control Protocol (XCP) [13, 15, 21], JetMax [37] and MaxNet [35]. Explicit congestion control protocols can convey accurate information to end-systems, which are then able

to better regulate their flow and congestion control mechanisms. In the class of explicit feedback algorithms, the Rate Control Protocol (RCP) [2, 6, 17] has the potential to offer stable and fair network performance, along with low latency and high link utilization. One architecture that could benefit from the use of RCP is a host-centric one, i.e., IP-based networks (for example, see [3, 30] and [33]). Another architecture that appears to be appealing for RCP are future data-centric networks, which are called Named Data Networking (NDN) [36]. In NDN, there is no IP address, and all data are named with unique names. Also, the data can be retrieved through multiple paths from multiple sources. In fact, the implicit feedback mechanism used by TCP is not reliable in these environments [28]. Therefore, researchers tend to focus on employing rate-based RCP-style algorithms in NDN; for e.g., see [20, 23] and [39].

RCP aims to achieve processor sharing by assigning a single fair rate for all the flows traversing the bottleneck link. The dynamics and performance of a protocol are largely affected by the mechanisms that routers employ to control the congestion. Currently, regardless of networking architectures, RCP computes the fair rate using two forms of feedback: rate mismatch and the queue size. An outstanding question in the design of RCP is whether two forms of feedback are needed in the protocol specification. We address this question by evaluating the performance of RCP with and without two forms of feedback. Early results in [17] show that the presence of queue feedback in RCP may lead to less accurate control over the queue size. However, this insight was based on some initial simulations, and more analysis would be required before arriving at a better understanding of this design consideration. An RCP router utilizes a field in the packet header to convey the fair share rate at which the flows can send data into the network. However, the feedback about the fair rate to end-systems is not instantaneous. Therefore, RCP works like a closed-loop control system with feedback delays. Hence, the stability becomes an important consideration in the design of RCP. Apart from ensuring stability, another important design objective is to make sure that the system converges quickly to a stable equilibrium. Therefore, we explore the impact of queue feedback on the local stability and the convergence properties of RCP. It is also natural to investigate the nature of instabilities that may occur if the stability conditions are just violated. We hasten to add that we are not interested in destabilizing the network, but wish to employ the tools offered by local instability analysis to gain some insights into the non-linear properties of the system under consideration. Thus, we also conduct a detailed local Hopf bifurcation analysis to investigate the effects of queue feedback on the non-linear dynamical properties of RCP. Taken together, we consider local stability, convergence rate, the type of Hopf bifurcation, and the stability of limit cycles as the performance metrics to deduce whether the queue feedback is beneficial or not.

In a control theoretic approach, congestion control algorithms are often modeled as delay differential equations. The systems with and without feedback based on queue size give rise to different nonlinear delay differential equations. For now, we consider the RCP model that assumes flows with the same round-trip time, operating over a single bottleneck link. Here, round-trip time (RTT)

denotes the sum of all the delays from source to link, and from link to source. Instability in the system could be induced by varying some of the system parameters. But, variations of some system parameters may affect the equilibrium values, which is undesirable. Moreover, to conduct a unified analysis of both the design choices, it is desirable to use a common exogenous parameter to push the system just into the unstable regime.

Previous studies of the stability of RCP were confined to developing sufficient conditions to ensure local stability [2, 17]. In this work, we derive necessary and sufficient conditions to ensure local asymptotic stability of RCP for the cases with and without queue size feedback. This enables us to determine the stability region in the parameter space. It is then shown that, as the bifurcation parameter varies, the system where feedback is based on both rate mismatch and queue size, readily loses local stability through a Hopf bifurcation [11]. Similarly, the rate of convergence analysis reveals that the convergence rate to equilibrium increases when the queue size term is absent. The theoretical framework we employ to study the nature of the Hopf bifurcations is the Poincaré normal form [11] which requires the computation of a center manifold existing near the degenerate equilibrium point under investigation and the determination of the flow on this manifold. Using this framework, we analytically characterize the type of Hopf bifurcation, and the nature of the bifurcating limit cycles. In [34], it was shown that the RCP which uses only rate mismatch feedback always exhibit a super-critical Hopf bifurcation, and the emerging limit cycles are asymptotically stable. So far, the bifurcation properties for the case where we have both rate mismatch and queue size feedback have not been studied. In this paper, we show that the RCP which uses both rate mismatch and queue size feedback can exhibit a sub-critical Hopf bifurcation, for some parameter values. A sub-critical Hopf bifurcation is undesirable for real engineering systems as a small perturbation around the system equilibrium may give rise to either limit cycles with large amplitude, or unstable limit cycles [32]. Thus, the queue feedback in the RCP model could create adverse effects on the stability of the limit cycles.

To the best of our knowledge, this is the *first study* that presents strong evidence to suggest that fluid models representing Internet congestion control algorithms can undergo a sub-critical Hopf bifurcation, for some parameter values. Therefore, this study reveals some novel insights into the non-linear dynamical properties which has been overlooked in previous studies of congestion control algorithms. Moreover, in general, the insights from Hopf bifurcation analysis could guide design considerations such that any loss of local stability only occurs via the emergence of small amplitude stable limit cycles. In other words, the nature of Hopf bifurcation and the stability of the bifurcating limit cycles should also be considered while designing congestion control protocols. Hence, this work could serve as an important step towards better design guidelines of the Internet congestion control algorithms. In essence, all the analytical results of this study tend to favor the design choice that uses only rate mismatch feedback. For such a system, a necessary and sufficient condition for non-oscillatory convergence is derived. This condition helps in finding an optimal value for

a key protocol parameter. Bifurcation diagrams, numerical computations and packet-level simulations serve to validate some of the theoretical insights.

The rest of this paper is structured as follows. In Section 2, we outline the non-linear fluid model for RCP. In Section 3, we investigate the local stability of RCP in the presence and absence of queue size feedback. The rate of convergence and local Hopf bifurcation analysis are outlined in Sections 4 and 5. A necessary and sufficient condition for non-oscillatory convergence is derived in Section 6. Finally, in Section 7, we summarize our key insights and suggest some avenues for further research.

2. RCP Model

At the fluid level, modeling the congestion control algorithms using the framework of delay differential equations has enabled their analysis to be subjected to tools from control and bifurcation theory. This section describes the non-linear model that represents the dynamics of the RCP protocol. RCP calculates the fair rate for all flows sharing a single bottleneck link by using feedback based on rate mismatch and the instantaneous queue size. The model for RCP is governed by the following non-linear delay differential equation [6, 34]

$$\frac{d}{dt}R(t) = \frac{R(t)}{C\overline{T}}\left(a\big(C - y(t)\big) - \beta\frac{q(t)}{\overline{T}}\right), \tag{1}$$

where

$$\begin{aligned} y(t) &= \sum_s R(t - T_s), \\ \frac{d}{dt}q(t) &= \begin{cases} \big[y(t) - C\big] & q(t) > 0 \\ \big[y(t) - C\big]^+ & q(t) = 0, \end{cases} \end{aligned} \tag{2}$$

using the notation $z^+ = \max(z, 0)$. Here $R(t)$ denotes the rate that RCP updates for all flows passing through the link, $y(t)$ is the aggregate load arriving at the link, C is the capacity of the link, $q(t)$ is the instantaneous queue size, T_s is the round-trip time (RTT) experienced by the traffic flow s, $\overline{T}$ represents the average RTT of packets passing through the link, and a, β are non-negative dimensionless protocol parameters.

The equation for the queue dynamics is

$$\frac{d}{dt}q(t) = \big[y(t) - C\big] \qquad \forall\ q\,(t)\,. \tag{3}$$

3. Local stability analysis

The initial, and in fact very common, style of stability analysis for non-linear time delayed systems is to first linearize the equation and then study the stability properties of the linearized system. In this section, the non-linear fluid model

of RCP is first linearized about its equilibrium, and then attractive conditions for local stability guide design recommendations. For the sake of simplicity, it is assumed that the bottleneck link carries flows with the same round-trip time τ. It is preferable not to use any of the system parameters as the bifurcation parameter, as varying them would affect the system equilibrium. Instead, an exogenous non-dimensional parameter, κ, is used to drive the system just into the regime of local instability. This has various advantages. we need not be concerned with the dimension of the parameter, and as it is common for both the design choices we can compare the results fairly.

3.1. Feedback based on rate mismatch and queue size

The RCP model under consideration can now be represented as

$$\begin{aligned} \frac{d}{dt}R(t) &= \frac{\kappa R(t)}{C\tau}\left(a\big(C - R(t-\tau)\big) - \beta\frac{q(t)}{\tau}\right), \\ \frac{d}{dt}q(t) &= \kappa\big(R(t-\tau) - C\big). \end{aligned} \tag{4}$$

Let (R^*, q^*) represents the non-trivial equilibrium of (4), then

$$\begin{aligned} R^* &= C, \\ q^* &= 0. \end{aligned} \tag{5}$$

From (5), it can be noted that the equilibrium values are independent of the bifurcation parameter κ. To linearize a non-linear system, we write the Taylor series expansion about the equilibrium point and include only the linear terms. Consider the perturbation $r(t) = R(t) - R^*$, and linearize (4) about the equilibrium to obtain

$$\begin{aligned} \frac{d}{dt}r(t) &= -\kappa\left(\frac{a}{\tau}r(t-\tau) + \frac{\beta}{\tau^2}q(t)\right), \\ \frac{d}{dt}q(t) &= \kappa r\left(t-\tau\right). \end{aligned} \tag{6}$$

The characteristic equation for the linearized system (6) is

$$\lambda^2\tau^2 e^{\lambda\tau} + a\kappa\tau\lambda + \kappa^2\beta = 0. \tag{7}$$

By analyzing the roots of the above transcendental characteristic equation, we proceed to derive a necessary and sufficient condition for local asymptotic stability. For the system to be stable, all the roots of (7) should lie on the open left-half, $\mathbf{Re}(\lambda) < 0$, of the complex plane. The system becomes locally unstable when the roots cross the imaginary axis and go to the right half of the complex plane. Therefore, the condition for the crossover defines the bounds on the model parameters which guarantees local asymptotic stability. To find the critical value of κ, at which the characteristic equation (7) has a pair of purely

imaginary roots, substitute $\lambda = i\omega_0,\ \omega_0 > 0$ in (7). Then, separating real and imaginary terms, and equating them to zero gives

$$-(\omega_0\tau)^2\cos(\omega_0\tau) + \kappa^2\beta = 0, \tag{8}$$

$$-(\omega_0\tau)^2\sin(\omega_0\tau) + \kappa a\omega_0\tau = 0. \tag{9}$$

Solving (8) and (9), yields

$$\kappa = \frac{1}{\theta}\sin^{-1}\left(\frac{a}{\theta}\right), \tag{10}$$

where

$$\theta = \frac{\omega_0\tau}{\kappa} = \sqrt{\frac{a^2 + \sqrt{a^4 + 4\beta^2}}{2}}. \tag{11}$$

Now, the critical value (κ_c) at which (7) has a purely imaginary root is given by

$$\kappa_c = \frac{1}{\sqrt{\frac{a^2+\sqrt{a^4+4\beta^2}}{2}}}\sin^{-1}\left(\frac{a}{\sqrt{\frac{a^2+\sqrt{a^4+4\beta^2}}{2}}}\right). \tag{12}$$

To exhibit that the system loses local asymptotic stability via a Hopf bifurcation, as κ increases beyond κ_c, the following transversality condition [11] has to be verified:

$$\mathbf{Re}\left(\frac{d\lambda}{d\kappa}\right)_{\kappa=\kappa_c} \neq 0.$$

Differentiating (7) with respect to κ gives

$$\frac{d\lambda}{d\kappa} = \frac{\lambda(a\lambda\tau + 2\kappa\beta)}{(2+\lambda\tau)(a\kappa\lambda\tau + \kappa^2\beta) - \kappa a\lambda\tau}.$$

It is clear that

$$\text{Sign}\left(\mathbf{Re}\left(\frac{d\lambda}{d\kappa}\right)\right)_{\kappa=\kappa_c} = \text{Sign}\left(\mathbf{Re}\left(\left(\frac{d\lambda}{d\kappa}\right)^{-1}\right)\right)_{\kappa=\kappa_c}.$$

Therefore, instead of finding $(d\lambda/d\kappa)$, consider its inverse, i.e., $(d\lambda/d\kappa)^{-1}$. Further simplification gives

$$\left(\frac{d\lambda}{d\kappa}\right)^{-1} = \kappa\left(\frac{1}{\lambda} + \frac{\tau(a\lambda\tau + \kappa\beta)}{(a\lambda\tau + 2\kappa\beta)}\right). \tag{13}$$

Evaluating the real part of (13) at $\kappa = \kappa_c$ yields

$$\left(\mathbf{Re}\left(\frac{d\lambda}{d\kappa}\right)^{-1}\right)_{\kappa=\kappa_c} = \kappa_c\tau\left(\frac{a^2\omega_0^2\tau^2 + 2\kappa_c^2\beta^2}{a^2\omega_0^2\tau^2 + 4\kappa_c^2\beta^2}\right) > 0,$$

which satisfies the transversality condition. The positivity of the above derivative implies that the system transits from stability to instability through a Hopf bifurcation, at $\kappa = \kappa_c$. It also means that the roots of (7) crossover the imaginary axis from left to right with positive velocity, and hence the system does not regain the stability with a further increase in κ. The linearized system (6) is asymptotically stable for all values of κ less than κ_c, and unstable for $\kappa > \kappa_c$. Now, the necessary and sufficient condition for local stability of (4) is

$$\kappa\theta < \sin^{-1}\left(\frac{a}{\theta}\right). \tag{14}$$

By setting $\kappa = 1$ (to get back to the original system), (14) can be rewritten as

$$\sqrt{\frac{a^2 + \sqrt{a^4 + 4\beta^2}}{2}} < \sin^{-1}\left(\frac{a}{\sqrt{\frac{a^2+\sqrt{a^4+4\beta^2}}{2}}}\right). \tag{15}$$

From (15), it can be observed that the protocol parameters a and β play a vital role in ensuring system local stability. Figure 1 graphically represents the Hopf condition and the region of local stability of RCP. This makes it easier to understand the relationship between a and β to ensure stability.

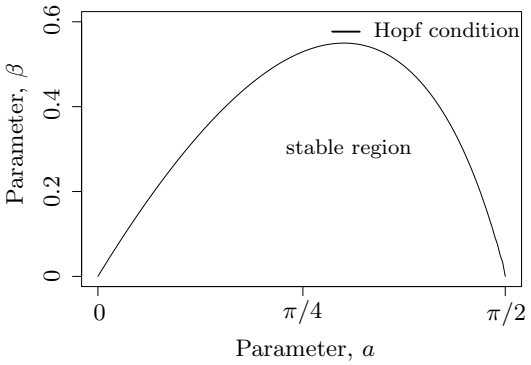

Figure 1: Local stability chart for (4), highlighting the relationship between the protocol parameters a and β to ensure local stability.

3.2. Feedback based on only rate mismatch

In this subsection, local stability analysis is performed for RCP which uses only rate mismatch feedback. To remove the queue term from the RCP model, β is set to zero in (4). This gives

$$\frac{d}{dt}R(t) = \frac{\kappa R(t)}{C\tau}\left(a\big(C - R(t-\tau)\big)\right). \tag{16}$$

Linearizing (16) about its equilibrium gives

$$\frac{d}{dt}r(t) = -\kappa\left(\frac{a}{\tau}r(t-\tau)\right). \tag{17}$$

The characteristic equation of (17) can be written as

$$\lambda + \left(\frac{\kappa a}{\tau}\right)e^{-\lambda\tau} = 0. \tag{18}$$

Proceeding as outlined in the previous subsection, the necessary and sufficient condition for local asymptotic stability of (16) can be written as

$$a\kappa < \frac{\pi}{2}. \tag{19}$$

Substituting $\kappa = 1$ gives

$$a < \frac{\pi}{2}. \tag{20}$$

Impact of queue size feedback on stability: As compared to (15), the RCP model which uses only rate mismatch feedback gives a simple stability condition, which makes it easier to design and ensure a stable system. It should be noted that condition (20) is necessary but not sufficient for the system (4) to be locally stable. Now, if the value of protocol parameter $a \in (0, \frac{\pi}{2})$, then the RCP system with no queue size feedback is locally stable, whereas the system with queue feedback loses its local stability through a Hopf bifurcation, as parameter b varies beyond some threshold. The Hopf bifurcation would lead to the emergence of limit cycles in the system dynamics. These limit cycles can manifest themselves in the queue size, which could degrade performance. Hence, the presence of queue size feedback seems to be detrimental to the system stability. A numerical example is now given to illustrate the existence of Hopf bifurcation and the emergence of limit cycles.

Numerical Example: Let $a = 1.5$, $\beta = 0.1$, $C = 1$ and $\tau = 1$. For these parameter values, using the Hopf condition (12), the critical value of the bifurcation parameter that drives the system to the edge of the stable regime is $\kappa_c = 1$. If κ goes beyond this critical value, the system will lose its local stability via a Hopf bifurcation which leads to the emergence of limit cycles. To verify this, the phase portraits of (4) for the cases: $\kappa < \kappa_c$ and $\kappa > \kappa_c$ are plotted in Figure 2. Using (5), we obtain the non-zero equilibrium of the system with the above choice of parameter values as $R^* = 1$. Based on the analytical results, for the value of $\kappa = 0.95 < \kappa_c$, the system should be locally stable. Indeed, as shown in Figure 2 (a), it can be observed that the rate $R(t)$ converges to the stable equilibrium (R^*), which implies that the system is locally asymptotically stable. We now marginally increase κ beyond κ_c (set $\kappa = 1.05$), thus pushing the system into the unstable region. As expected, the system exhibits limit cycles (see Figure 2 (b)). The numerical simulations were done using the numerical computing software MATLAB. The bifurcation diagram shown in Figure 3 was drawn using the MATLAB package DDE-Biftool [7, 8]. Figure 3 shows the existence of a super-critical Hopf as the bifurcation parameter κ increases beyond κ_c.

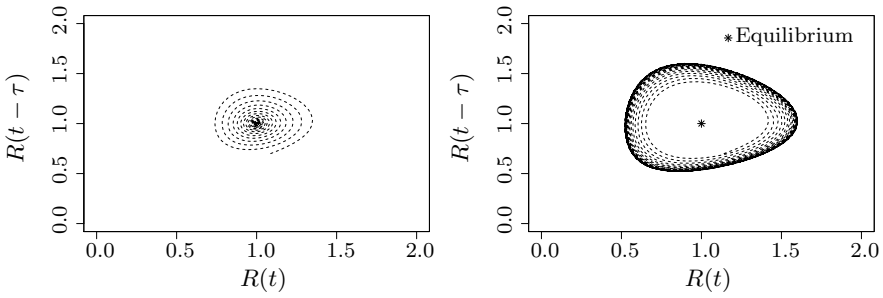

(a) $\kappa = 0.95$ (b) $\kappa = 1.05$

Figure 2: Phase portraits of equation (4) highlighting (a) convergence of the rate to a stable equilibrium, $R^* = 1$ for $\kappa = 0.95$, and (b) existence of a stable limit cycle for $\kappa = 1.05$. As κ increases beyond the critical value, the system dynamics exhibits a qualitative change from a stable fixed point to a limit cycle. The values of the parameters used are $a = 1.5$, $\beta = 0.1$, $C = 1$ and $\tau = 1$.

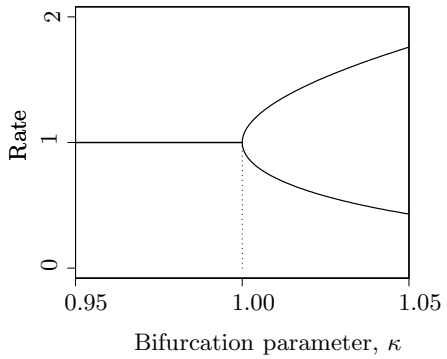

Figure 3: Bifurcation diagram showing the emergence of limit cycles as the bifurcation parameter κ increases beyond 1. The parameter values used are $a = 1.5$, $\beta = 0.1$, $C = 1$ and $\tau = 1$. For theses parameter values, the critical value at which Hopf occurs is $\kappa = 1$.

Another essential compliment to the theoretical analysis is the packet-level simulations. The theoretical insights should be validated by investigating if the packet-level simulations of the underlying system exhibits the qualitative properties predicted through the analysis of the fluid model. The packet-level simulations are done using a discrete event RCP simulator (for more details, refer to [17]). The simulated network has a single bottleneck link setup that considers $C = 1$ packet per unit time, number of flows = 100 and RTT of all the flows as $\tau = 100$ time units. Simulation traces in Figure 4 (a) and Figure 4 (b) show the evolution of queue size for the choice of parameter values $a = 0.5$, $\beta = 1$ and $a = 0.5$, $\beta = 0$, respectively. From (20), for the choice $a = 0.5$, $\beta = 0$, the system is expected to be stable. Indeed, this is confirmed in the simulation traces in Figure 4 (a) which does not exhibit any limit cycles in the queue size. Figure 4 (b) shows the emergence of limit cycles in the queue size. This is as expected, since the parameter values $a = 0.5$ and $\beta = 1$ violates the stability condition (15), and lies outside the stable region (see Figure 1).

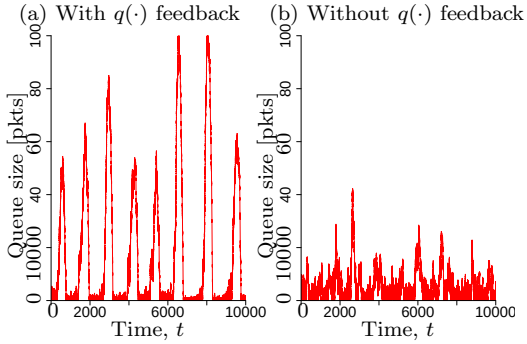

Figure 4: Traces from a packet-level simulation showing the evolution of queue size in a single bottleneck link with $C = 1$ packet per unit time, $\tau = 100$ time units and 100 RCP sources. Observe that the queue appears to be stable for the choice of parameter values $a = 0.5$ and $\beta = 0$, whereas it begins to oscillate for $a = 0.5$ and $\beta = 1$.

4. Rate of convergence

We now consider some convergence properties of the system in the stable regime. Rate of convergence is a key performance metric which must be considered for a congestion control algorithm. To that end, the impact of queue feedback on the convergence rate is examined by conducting the rate of convergence analysis in the presence and absence of queue size feedback.

4.1. Feedback based on rate mismatch and queue size

To recapitulate, the characteristic equation of the linearized model of RCP which uses both rate mismatch and queue size feedback is

$$\lambda^2\tau^2 e^{\lambda\tau} + a\tau\lambda + \beta = 0. \tag{21}$$

From (21) it can be observed that the characteristic function corresponding to the system is a second order quasi-polynomial. Therefore, in this case, it is difficult to get closed-form analytical expressions for the rate of convergence. In such a case, we resort to some numerical computation tools that can assist in finding the rightmost root of the characteristic equation. The real part of the rightmost root can give insights about the system behavior, and it can be used to calculate the rate of convergence. We use DDE-Biftool to analyze the rate of convergence for the system which includes queue feedback. For delay differential equations with real coefficients, the rightmost root could be a single real root or a complex conjugate pair. Figure 5 shows the rate of convergence computed numerically using DDE-Biftool, for various values of the protocol parameters. From Figure 5, we can observe that the rate of convergence decreases as the value of β increases. The parameter values chosen are $C = 10$ and $\tau = 1$.

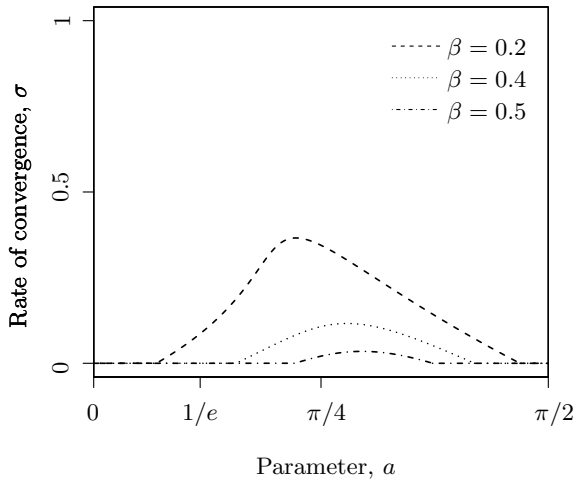

Figure 5: Convergence rate to equilibrium of RCP for various values of the protocol parameter β. It can be observed that the rate of convergence decreases as the value of β increases. The parameter values used are $C = 10$ and $\tau = 1$.

4.2. Feedback based on only rate mismatch

In this section, following the style of analysis outlined in [4], the rate of convergence analysis is performed for the RCP which uses only rate mismatch feedback. The analytical results enable us to investigate the impact of protocol parameters on the convergence rate. Here, we consider $\kappa = 1$, to get back the original system. Now the characteristic equation can be written as

$$\lambda + \left(\frac{a}{\tau}\right) e^{-\lambda\tau} = 0. \tag{22}$$

Substituting $\lambda\tau = x - \sigma\tau$ in (22) yields

$$(\sigma\tau - x)e^x - ae^{\sigma\tau} = 0. \tag{23}$$

Here, σ is considered to be the supremum of the solutions of (23) over $(0, \infty)$ which guarantees that all the characteristic roots lie on the open left half of the complex plane. Let $-\alpha < 0$ be the largest real part of all the roots of (23). Then, the rate at which the system approaches a stable equilibrium is given by $\sigma = (\alpha/\tau)$. A necessary and sufficient condition for all the eigenvalues of (23) to lie on the left half-plane is [12]

$$\sigma\tau < 1, \tag{24}$$

$$\sigma\tau < ae^{\sigma\tau}, \tag{25}$$

$$ae^{\sigma\tau} < \frac{u}{\sin(u)}, \tag{26}$$

where u is the solution of the equation

$$u = \sigma\tau \tan(u), \tag{27}$$

in $0 < u < \pi$, with $u = \pi/2$ if $\sigma = 0$. Consider the following function

$$g(u) = \frac{u}{\sin(u)} e^{-u/\tan(u)}, \tag{28}$$

which increases monotonically in the interval $u \in (0, \pi)$, with $g(0) = 1/e$, $g(\pi/2) = \pi/2$ and $\lim_{u\to\pi}\ g(u) = \infty$. Now, using (27) and (28), the inequality (26) can be rewritten as

$$a < g(u). \tag{29}$$

As σ increases, u decreases, and hence $g(u)$ is decreasing function of σ. Therefore, the maximum value of σ that satisfies (29) can be obtained by solving its corresponding equality. By a similar argument, the left hand side of (24) and (25) increases with increase in σ. Thus, the maximum value of σ that satisfies the inequalities (24), (25) can be determined by solving the corresponding equalities. If the solution does not exist for any of these equations, then there is no restriction on the value of σ. Now, we summarize the results as follows. Let σ_1, σ_2, σ_3 be the solutions of

$$\sigma\tau = 1, \tag{30}$$

$$\sigma\tau e^{-\sigma\tau} = a, \tag{31}$$

$$u = \sigma\tau \tan(u), \quad g(u) = a, \tag{32}$$

respectively. Consider $\sigma_i = \infty$, for $i = 1,\ 2,\ 3$ if there is no solution exists for the corresponding equality. Then, the convergence rate σ is given by

$$\sigma = \min[\sigma_1, \sigma_2, \sigma_3]. \tag{33}$$

Now, the next step is to analyze the dependence of convergence rate on protocol parameter a, for $\tau > 0$. The function $\sigma\tau e^{-\sigma\tau}$ reaches its maximum value of $1/e$ at $\sigma\tau = 1$. Similarly the function $g(u)$ has a minima of $1/e$ at $u = 0$. Let $a^* = 1/e$, then there is no solution for (31) if $a > a^*$, and for (32) if $a < a^*$. Let σ_2 be the solution of (31) on $0 < a \leq a^*$. Similarly, consider σ_3 be the solution of (32) on $a > a^*$. At $a = 0$, it is obvious that the rate of convergence $\sigma = 0$.

Case 1 : $a \in (0, a^*)$. Differentiating (31) with respect to a gives

$$\frac{d\sigma}{da} = \frac{e^{\sigma\tau}}{\tau(1 - ae^{\sigma\tau})}. \tag{34}$$

Using (31), the derivative (34) can be written as

$$\frac{d\sigma}{da} = \frac{e^{\sigma\tau}}{\tau(1 - \sigma\tau)}. \tag{35}$$

From (35), it can deduced that $d\sigma_2/da > 0$ if $\sigma_2\tau < 1$. Hence $\sigma_2 < \sigma_1$ for $a \in (0, a^*)$.

Case 2 : $a = a^*$. Substituting $a = a^* = 1/e$ in (31) yields

$$\sigma_2\tau e^{-\sigma_2\tau} = a = 1/e. \tag{36}$$

It is known that the function $\sigma_2\tau e^{-\sigma_2\tau}$ reaches maximum of $1/e$ at $\sigma_2\tau = 1$, thus $\sigma_2 = \sigma_1 = 1/\tau$ at $a = a^*$.

Case 3 : $a > a^*$. For $a > a^*$, using (32), the following holds

$$g(u) = \frac{u}{\sin(u)} e^{-u/\tan(u)} > 1/e. \tag{37}$$

For $u \in (0, \pi)$ and $u/\sin(u) > 1$, (37) can be written as

$$e^{-u/\tan(u)} > 1/e. \tag{38}$$

From (38), it can be deduced that $u/\tan(u) < 1$, and hence $\sigma_3\tau < 1$, and $\sigma_3 < \sigma_1$.

To summarize, the convergence rate σ is given by

$$\sigma = \min[\sigma_1, \sigma_2] = \sigma_2 \quad a \in (0, a^*], \tag{39}$$

$$= \min[\sigma_1, \sigma_3] = \sigma_3 \quad a > a^*, \tag{40}$$

where $a^* = 1/e$. Figure 6 shows the variation of convergence rate with protocol parameter a for various values of τ. It can observed that the rate of convergence increases with a for $a < 1/e$, and decreases when $a > 1/e$. Also, the convergence rate is maximum at $a = (1/e)$, so the optimal value of the protocol parameter for fast convergence is $a = (1/e)$. Also, the rate of convergence decreases with an increase in the round-trip time (see Figure 7). The numerical simulations shown in Figure 7 are done using the computing software XPPAUT [9].

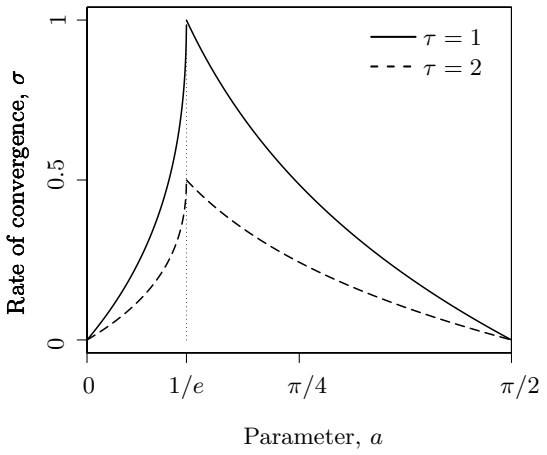

Figure 6: Rate of convergence to equilibrium for RCP without queue feedback. The rate of convergence increases with a and reaches maxima of $1/\tau$ at $a = 1/e$, and then decreases for $a > 1/e$.

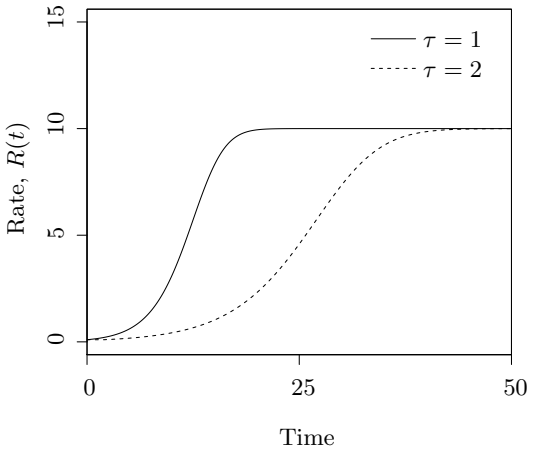

Figure 7: Numerical simulations of RCP without queue feedback, highlighting the decrease in convergence rate as RTT increases. The parameter values used are $C = 10$ and $a = 1/e$.

For the sake of comparison, the rate of convergence for the case $b > 0$ is also shown in Figure 8. As can be observed from Figure 8, the removal of queue size feedback from RCP improves the convergence rate to equilibrium. Numerical simulations in Figure 9 serve to validate the analytical insights.

However, rather than being confined to a stable regime, it is also worth investigating the behavior of the protocol if the system becomes unstable. Therefore, in the next section, we analyze the consequences associated with the loss of stability for both the design choices.

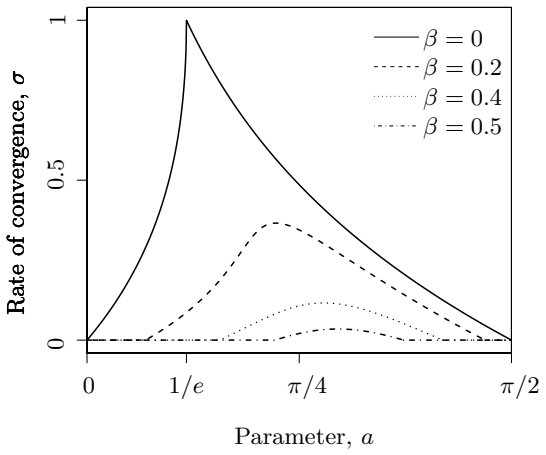

Figure 8: Convergence rate to equilibrium of RCP for various values of the protocol parameter β. We can observe that the convergence rate can be improved by excluding the queue size feedback. The parameter values used are $C = 10$ and $\tau = 1$.

5. Local Hopf bifurcation analysis

In the previous sections, we analyzed local stability and convergence properties of the RCP protocol. The next natural step is to investigate the dynamical behavior of the system as it transits from a stable to an unstable regime. In this section, we explore the impact of loss of local stability for both the design options, i.e., with and without queue size feedback. In the bifurcation-theoretic analysis, we have to take non-linear terms into consideration, which helps to learn additional non-linear dynamical properties of the system with and without queue size feedback.

5.1. With queue feedback

In the local Hopf bifurcation analysis, we use the theoretical framework of Poincarè normal forms and the center manifold theorem to investigate the type

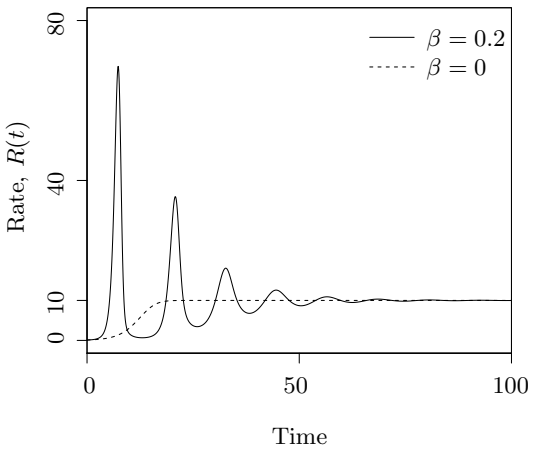

Figure 9: Numerical simulations highlighting that the system can converge to its equilibrium ($R^* = 10$) much faster, if the queue size feedback is not included in the RCP. The parameter values used are $C = 10$, $a = 1/e$ and $\tau = 1$.

of Hopf bifurcation and the asymptotic orbital stability of the bifurcating limit cycles. For our study, we closely follow the style of analysis provided in [11].

We start by conducting a Taylor series expansion of (4) about the equilibrium, to get

$$\begin{aligned} \frac{d}{dt}r(t) &= -\kappa\left(\frac{a}{\tau}r(t-\tau) + \frac{\beta}{\tau^2}q(t) + \frac{a}{C\tau}r(t)r(t-\tau) + \frac{\beta}{C\tau^2}r(t)q(t)\right), \\ \frac{d}{dt}q(t) &= \kappa r(t-\tau). \end{aligned} \tag{41}$$

At $\kappa = \kappa_c$, the system satisfies the Hopf bifurcation condition, and a further increase in κ would drive the system into the unstable region. Let $\kappa = \kappa_c + \mu$, where $\kappa_c = 1$, and the Hopf bifurcation takes place at $\mu = 0$.

Consider the following autonomous delay-differential system

$$\frac{d}{dt}\boldsymbol{u}(t) = \mathcal{L}_\mu \boldsymbol{u}_t + \mathcal{F}(\boldsymbol{u}_t, \mu) \tag{42}$$

where $t > 0$, $\mu \in \mathbb{R}$, $\tau > 0$,

$$\boldsymbol{u}_t(\theta) = \boldsymbol{u}(t+\theta), \qquad \boldsymbol{u} : \big[-\tau, 0\big] \to \mathbb{R}^2, \qquad \theta \in [-\tau, 0].$$

$\mathcal{L}_\mu$ is a one-parameter family of continuous (bounded) linear operators. The operator $\mathcal{F}(\boldsymbol{u}_t, \mu)$ contains the non-linear terms. We assume that $\mathcal{F}$ and $\mathcal{L}_\mu$ depend analytically on the bifurcation parameter μ for small $|\mu|$. Note that

(41) is of the form (42), where $\boldsymbol{u} = \big[r, q\big]^T$, and

$$\begin{aligned}\mathcal{L}_\mu \boldsymbol{\phi} = &\quad \kappa \begin{bmatrix} 0 & -\frac{\beta}{\tau^2} \\ 0 & 0 \end{bmatrix} \boldsymbol{\phi}(0) + \kappa \begin{bmatrix} -\frac{a}{\tau} & 0 \\ 1 & 0 \end{bmatrix} \boldsymbol{\phi}(-\tau), \\ \mathcal{F}(\boldsymbol{u}_t, \mu) = &-\kappa \begin{bmatrix} \frac{a}{C\tau} r(t) r(t-\tau) + \frac{\beta}{C\tau^2} r(t) q(t) \\ 0 \end{bmatrix}.\end{aligned}$$

The objective now is to cast (42) into the form which has $\boldsymbol{u}_t$ instead of both $\boldsymbol{u}$ and $\boldsymbol{u}_t$, i.e.,

$$\frac{d}{dt}\boldsymbol{u}_t = \mathcal{A}(\mu)\boldsymbol{u}_t + \mathcal{R}\boldsymbol{u}_t. \tag{43}$$

First, transform the linear problem $d\boldsymbol{u}(t)/dt = \mathcal{L}_\mu \boldsymbol{u}_t$. By Riesz representation theorem, there exists a 2×2 matrix function $\eta(\cdot, \mu) : [-\tau, 0] \to \mathbb{R}^{2\times 2}$, such that the components of η have bounded variation and for all $\boldsymbol{\phi} \in C[-\tau, 0]$

$$\mathcal{L}_\mu \boldsymbol{\phi} = \int_{-\tau}^{0} \mathrm{d}\eta(\theta, \mu)\boldsymbol{\phi}(\theta).$$

In particular,

$$\mathcal{L}_\mu \boldsymbol{u}_t = \int_{-\tau}^{0} \mathrm{d}\eta(\theta, \mu)\boldsymbol{u}(t+\theta). \tag{44}$$

Observe that

$$\mathrm{d}\eta(\theta, \mu) = \kappa \begin{bmatrix} -\frac{a}{\tau}\delta(\theta+\tau) & -\frac{\beta}{\tau^2}\delta(\theta) \\ \delta(\theta+\tau) & 0 \end{bmatrix} \mathrm{d}\theta \tag{45}$$

satisfies (44). Here, $\delta(\theta)$ is the Dirac delta function. For $\boldsymbol{\phi} \in C^1\big[-\tau, 0\big]$, define

$$\mathcal{A}(\mu)\boldsymbol{\phi}(\theta) = \begin{cases} \frac{\mathrm{d}\boldsymbol{\phi}(\theta)}{\mathrm{d}\theta}, & \theta \in [-\tau, 0), \\ \int_{-\tau}^{0} \mathrm{d}\eta(s, \mu)\boldsymbol{\phi}(s) \equiv \mathcal{L}_\mu \boldsymbol{\phi}, & \theta = 0, \end{cases} \tag{46}$$

and

$$\mathcal{R}\boldsymbol{\phi}(\theta) = \begin{cases} 0, & \theta \in [-\tau, 0), \\ \mathcal{F}(\boldsymbol{\phi}, \mu), & \theta = 0. \end{cases} \tag{47}$$

As $\mathrm{d}\boldsymbol{u}_t/\mathrm{d}\theta = \mathrm{d}\boldsymbol{u}_t/\mathrm{d}t$, (42) becomes (43) as desired. Let $\boldsymbol{q}(\theta)$ be the eigenfunction for $\mathcal{A}(0)$ corresponding to $\lambda(0)$,

$$\mathcal{A}(0)\boldsymbol{q}(\theta) = i\omega_0 \boldsymbol{q}(\theta). \tag{48}$$

To find ω_0 and $\boldsymbol{q}(\theta)$, let $\boldsymbol{q}(\theta) = \boldsymbol{q}_0 e^{i\omega_0\theta}$, where $\boldsymbol{q}_0 = [q_{01}, q_{02}]^T$. Now, using (48) and (46), and following the style of analysis done for the equations (8) and (9), we get

$$\begin{aligned} &\kappa a = (\omega_0\tau)\sin(\omega_0\tau), && \kappa^2\beta = (\omega_0\tau)^2\cos(\omega_0\tau), \\ &\boldsymbol{q}_0 = \begin{bmatrix} 1 \\ -\frac{i\omega_0\tau^2}{(\kappa\beta + ia\omega_0\tau)} \end{bmatrix} \equiv \begin{bmatrix} q_{01} \\ q_{02} \end{bmatrix}, && \omega_0 = \frac{\kappa}{\tau}\sqrt{\frac{a^2 + \sqrt{a^4 + 4\beta^2}}{2}}. \end{aligned} \tag{49}$$

Define the adjoint operator $\mathcal{A}^*(0)$ as

$$\mathcal{A}^*(0)\boldsymbol{\alpha}(s) = \begin{cases} -\frac{\mathrm{d}\boldsymbol{\alpha}(s)}{\mathrm{d}s}, & s \in (0,\tau], \\ \int_{-\tau}^{0} \mathrm{d}\eta^T(t,0)\boldsymbol{\alpha}(-t), & s = 0. \end{cases}$$

Note that the domains of $\mathcal{A}$ and $\mathcal{A}^*$ are $C^1[-\tau,0]$ and $C^1[0,\tau]$, respectively. As

$$\mathcal{A}(0)\boldsymbol{q}(\theta) = \lambda(0)\boldsymbol{q}(\theta)$$

$\overline{\lambda}(0)$ is an eigenvalue for $\mathcal{A}^*$, and

$$\mathcal{A}^*(0)\boldsymbol{q}^* = -i\omega_0\boldsymbol{q}^*$$

for some non-zero vector $\boldsymbol{q}^*$. Thus, we get

$$\boldsymbol{q}^* = \Omega \begin{bmatrix} 1 \\ \frac{\kappa\beta}{i\omega_0\tau^2} \end{bmatrix} \equiv \begin{bmatrix} q_{01}^* \\ q_{02}^* \end{bmatrix}, \tag{50}$$

where Ω is a non-zero scalar. For $\boldsymbol{\phi} \in C[-\tau,0]$ and $\boldsymbol{\psi} \in C[0,\tau]$, define an inner product

$$\langle \boldsymbol{\psi}, \boldsymbol{\phi} \rangle = \overline{\boldsymbol{\psi}}(0)\cdot\boldsymbol{\phi}(0) - \int_{\theta=-\tau}^{0}\int_{\zeta=0}^{\theta} \overline{\boldsymbol{\psi}}^T(\zeta-\theta)\mathrm{d}\eta(\theta)\boldsymbol{\phi}(\zeta)\mathrm{d}\zeta, \tag{51}$$

where $\boldsymbol{a}\cdot\boldsymbol{b}$ means $\sum a_i b_i$. Then, $\langle \boldsymbol{\psi}, \mathcal{A}\boldsymbol{\phi}\rangle = \langle \mathcal{A}^*\boldsymbol{\psi}, \boldsymbol{\phi}\rangle$ for $\boldsymbol{\phi} \in \mathrm{Dom}(\mathcal{A})$ and $\boldsymbol{\psi} \in \mathrm{Dom}(\mathcal{A})$. Using (51) to find Ω such that $\langle \boldsymbol{q}^*, \boldsymbol{q}\rangle = 1$, we get

$$1 = \overline{\Omega}\Big(1 + q_{02}\overline{q}_{02}^* + e^{-i\omega_0\tau}\left(\overline{q}_{02}^*\tau - \kappa a\right)\Big).$$

On simplification, we obtain

$$\Omega = \left(1 - i\omega_0\tau + \frac{\kappa\beta}{\kappa\beta - ia\omega_0\tau}\right)^{-1}. \tag{52}$$

Similarly, we can also verify that $\langle \boldsymbol{q}^*, \overline{\boldsymbol{q}}\rangle = 0$. For $\boldsymbol{u}_t$, a solution of (43) at $\mu = 0$, define

$$\begin{aligned} z(t) &= \langle \boldsymbol{q}^*, \boldsymbol{u}_t\rangle, \\ \boldsymbol{w}(t,\theta) &= \boldsymbol{u}_t(\theta) - 2\mathbf{Re}\left(z(t)\boldsymbol{q}(\theta)\right). \end{aligned}$$

Then, on the manifold, C_0, $\boldsymbol{w}(t,\theta) = \boldsymbol{w}\big(z(t),\overline{z}(t),\theta\big)$, where

$$\boldsymbol{w}\big(z,\overline{z},\theta\big) = \boldsymbol{w}_{20}(\theta)\frac{z^2}{2} + \boldsymbol{w}_{11}(\theta)z\overline{z} + \boldsymbol{w}_{02}(\theta)\frac{\overline{z}^2}{2} + \cdots. \tag{53}$$

In effect, z and $\overline{z}$ are local coordinates for C_0 in C in the directions of $\boldsymbol{q}^*$ and $\overline{\boldsymbol{q}}^*$, respectively. The existence of the center manifold enables the reduction of

(43) to an ordinary differential equation for a single complex variable on C_0. At $\mu = 0$, we get

$$\begin{aligned} z^{'}(t) &= \langle \boldsymbol{q}^*, \mathcal{A}\boldsymbol{u}_t + \mathcal{R}\boldsymbol{u}_t \rangle, \\ &= i\omega_0 z(t) + \overline{\boldsymbol{q}}^*(0) \cdot \mathcal{F}\Big(\boldsymbol{w}(z, \overline{z}, \theta) + 2\mathbf{Re}\Big(z\boldsymbol{q}(\theta) \Big) \Big), \\ &= i\omega_0 z(t) + \overline{\boldsymbol{q}}^*(0) \cdot \mathcal{F}_0(z, \overline{z}), \end{aligned} \tag{54}$$

which can be abbreviated as

$$z^{'}(t) = i\omega_0 z(t) + g\big(z, \overline{z}\big). \tag{55}$$

The next objective is to expand g in powers of z and $\overline{z}$. However, we also have to determine the coefficients $\boldsymbol{w}_{ij}(\theta)$ in (53). Once the coefficients $\boldsymbol{w}_{ij}$ are determined, the differential equation (54) for z would be explicit (as abbreviated in (54)). Expanding $g(z, \overline{z})$ in powers of z and $\overline{z}$, we have

$$\begin{aligned} g(z, \overline{z}) &= \overline{\boldsymbol{q}}^*(0) \cdot \mathcal{F}_0\big(z, \overline{z}\big), \\ &= g_{20}\frac{z^2}{2} + g_{11} z\overline{z} + g_{02}\frac{\overline{z}^2}{2} + g_{21}\frac{z^2\overline{z}}{2} \cdots . \end{aligned}$$

Following [11], we write

$$\boldsymbol{w}^{'} = u_t^{'} - z^{'}\boldsymbol{q} - \overline{z}^{'}\overline{\boldsymbol{q}},$$

and using (43) and (55) we obtain

$$\boldsymbol{w}^{'} = \begin{cases} \mathcal{A}\boldsymbol{w} - 2\mathbf{Re}\left(\overline{\boldsymbol{q}}^*(0) \cdot \mathcal{F}_0 \boldsymbol{q}(\theta) \right), & \theta \in [-\tau, 0), \\ \mathcal{A}\boldsymbol{w} - 2\mathbf{Re}\left(\overline{\boldsymbol{q}}^*(0) \cdot \mathcal{F}_0 q(0) \right) + \mathcal{F}_0, & \theta = 0, \end{cases}$$

which is rewritten as

$$\boldsymbol{w}^{'} = \mathcal{A}\boldsymbol{w} + \boldsymbol{h}\big(z, \overline{z}, \theta\big) \tag{56}$$

using (53), where

$$\boldsymbol{h}(z, \overline{z}, \theta) = \boldsymbol{h}_{20}(\theta)\frac{z^2}{2} + \boldsymbol{h}_{11}(\theta) z\overline{z} + \boldsymbol{h}_{02}(\theta)\frac{\overline{z}^2}{2} + \cdots . \tag{57}$$

On the manifold, C_0, near the origin

$$\boldsymbol{w}^{'} = \boldsymbol{w}_z z^{'} + \boldsymbol{w}_{\overline{z}}\overline{z}^{'}.$$

Using (53) and (55) to replace $\boldsymbol{w}_z$, $z^{'}$ (and their conjugates by their power series expansion) and equating this with (56), we get

$$\begin{aligned} \big(2i\omega_0 - \mathcal{A}\big)\boldsymbol{w}_{20}(\theta) &= \boldsymbol{h}_{20}(\theta), \\ -\mathcal{A}\boldsymbol{w}_{11}(\theta) &= \boldsymbol{h}_{11}(\theta), \\ -\big(2i\omega_0 + \mathcal{A}\big)\boldsymbol{w}_{02}(\theta) &= \boldsymbol{h}_{02}(\theta). \end{aligned} \tag{58}$$

Note that

$$\begin{aligned}\boldsymbol{u}_t(\theta) &= \boldsymbol{w}\big(z,\overline{z},\theta\big) + \boldsymbol{q}(\theta)z + \overline{\boldsymbol{q}}(\theta)\overline{z},\\ &= \boldsymbol{w}_{20}(\theta)\frac{z^2}{2} + \boldsymbol{w}_{11}(\theta)z\overline{z} + \boldsymbol{w}_{02}(\theta)\frac{\overline{z}^2}{2} + \boldsymbol{q}_0 e^{i\omega_0\theta}z + \overline{\boldsymbol{q}}_0 e^{-i\omega_0\theta}\overline{z} + \cdots,\end{aligned}$$

from which we obtain $\boldsymbol{u}_t(0)$ and $\boldsymbol{u}_t(-\tau)$. We need to find the coefficients of z^2, $z\overline{z}$, $\overline{z}^2$, $z^2\overline{z}$. Hence, we only keep these relevant terms in the expansions as follows:

$$\begin{aligned}r_t(0)q_t(0) &= q_{02}z^2 + \overline{q}_{02}\overline{z}^2 + \big(\overline{q}_{02} + q_{02}\big)z\overline{z} + \Bigg(\frac{w_{201}(0)\overline{q}_{02}}{2} + w_{111}(0)q_{02} + w_{112}(0)\\ &\quad + \frac{w_{202}(0)}{2}\Bigg)z^2\overline{z} + \cdots,\\ r_t(0)r_t(-\tau) &= e^{-i\omega_0\tau}z^2 + e^{i\omega_0\tau}\overline{z}^2 + \Big(e^{i\omega_0\tau} + e^{-i\omega_0\tau}\Big)z\overline{z} + \Bigg(\frac{w_{201}(0)e^{i\omega_0\tau}}{2}\\ &\quad + w_{111}(0)e^{-i\omega_0\tau} + w_{111}(-\tau) + \frac{w_{201}(-\tau)}{2}\Bigg)z^2\overline{z} + \cdots,\end{aligned} \tag{59}$$

where $[w_{ij1}, w_{ij2}]^T = \boldsymbol{w}_{ij}$. Recall that,

$$g(z,\overline{z}) = \overline{\boldsymbol{q}}^*(0)\cdot\mathcal{F}_0(z,\overline{z}), \tag{60}$$

where $[\mathcal{F}_{01}, \mathcal{F}_{02}]^T = \mathcal{F}_0$, and

$$g(z,\overline{z}) = g_{20}\frac{z^2}{2} + g_{11}z\overline{z} + g_{02}\frac{\overline{z}^2}{2} + g_{21}\frac{z^2\overline{z}}{2}\cdots. \tag{61}$$

Comparing (60) and (61), and using (59), we get

$$\begin{aligned}g_{20} &= -2\overline{\Omega}\kappa\left(\frac{a}{C\tau}e^{-i\omega_0\tau} + \frac{\beta}{C\tau^2}q_{02}\right),\\ g_{11} &= -\overline{\Omega}\kappa\left(\frac{a}{C\tau}\left(e^{i\omega_0\tau} + e^{-i\omega_0\tau}\right) + \frac{\beta}{C\tau^2}\left(\overline{q}_{02} + q_{02}\right)\right),\\ g_{02} &= -2\overline{\Omega}\kappa\left(\frac{a}{C\tau}e^{i\omega_0\tau} + \frac{\beta}{C\tau^2}\overline{q}_{02}\right),\end{aligned}$$

$$\begin{aligned}g_{21} = \overline{\Omega}\kappa\Bigg(&-\frac{a}{C\tau}\Big(w_{201}(-\tau) + 2w_{111}(-\tau) + w_{201}(0)e^{i\omega_0\tau} + 2w_{111}(0)e^{-i\omega_0\tau}\Big)\\ &- \frac{\beta}{C\tau^2}\Big(\overline{q}_{02}w_{201}(0) + 2q_{02}w_{111}(0) + w_{202}(0) + 2w_{112}(0)\Big)\Bigg).\end{aligned}$$

On further simplification, we obtain

$$g_{20} = \frac{2i\overline{\Omega}\omega_0}{C}, \qquad g_{11} = 0, \qquad g_{02} = \frac{-2i\overline{\Omega}\omega_0}{C},$$

$$g_{21} = -\frac{\overline{\Omega}}{C\tau}\Bigg(i\omega_0\tau w_{201}(0) + \kappa a w_{201}(-\tau) + \frac{\kappa\beta w_{202}(0)}{\tau} - 2i\omega_0\tau w_{111}(0) + 2\kappa a w_{111}(-\tau) + \frac{2\kappa\beta w_{112}(0)}{\tau}\Bigg).$$

For the expression of g_{21}, we still need to evaluate $\boldsymbol{w}_{11}(0)$, $\boldsymbol{w}_{11}(-\tau)$, $\boldsymbol{w}_{20}(0)$ and $\boldsymbol{w}_{20}(-\tau)$. Now for $\theta \in [-\tau, 0)$

$$\begin{aligned}\boldsymbol{h}(z,\overline{z},\theta) &= -2\mathbf{Re}\left(\overline{\boldsymbol{q}}^*(0)\cdot\mathcal{F}_0\boldsymbol{q}(\theta)\right),\\ &= -2\mathbf{Re}\left(g(z,\overline{z})\boldsymbol{q}(\theta)\right),\\ &= \left(g_{20}\frac{z^2}{2} + g_{11}z\overline{z} + g_{02}\frac{\overline{z}^2}{2}\right)\boldsymbol{q}(\theta) - \left(\overline{g}_{20}\frac{z^2}{2} + \overline{g}_{11}z\overline{z} + \overline{g}_{02}\frac{\overline{z}^2}{2}\right)\overline{\boldsymbol{q}}(\theta),\end{aligned}$$

which, when compared with (57), gives

$$\begin{aligned}\boldsymbol{h}_{20}(\theta) &= -g_{20}\boldsymbol{q}(\theta) - \overline{g}_{02}\overline{\boldsymbol{q}}(\theta),\\ \boldsymbol{h}_{11}(\theta) &= -g_{11}\boldsymbol{q}(\theta) - \overline{g}_{11}\overline{\boldsymbol{q}}(\theta) = 0.\end{aligned}$$

From (46) and (58), we get

$$\boldsymbol{w}_{20}^{'}(\theta) = 2i\omega_0\boldsymbol{w}_{20}(\theta) + g_{20}\boldsymbol{q}(\theta) + \overline{g}_{02}\overline{\boldsymbol{q}}(\theta), \tag{62}$$

$$\boldsymbol{w}_{11}^{'}(\theta) = 0. \tag{63}$$

Solving the differential equations (62) and (63), we obtain

$$\boldsymbol{w}_{20}(\theta) = -\frac{g_{20}}{i\omega_0}\boldsymbol{q}_0 e^{i\omega_0\theta} - \frac{\overline{g}_{02}}{3i\omega_0}\overline{\boldsymbol{q}}_0 e^{-i\omega_0\theta} + \boldsymbol{e}e^{2i\omega_0\theta}, \tag{64}$$

$$\boldsymbol{w}_{11}(\theta) = \boldsymbol{f}, \tag{65}$$

for some $\boldsymbol{e} = [e_1, e_2]^T$ and $\boldsymbol{f} = [f_1, f_2]^T$.
From $\boldsymbol{h}(z,\overline{z},0) = -2\mathbf{Re}\Big(\overline{\boldsymbol{q}}^*(0)\cdot\mathcal{F}_0\boldsymbol{q}(0)\Big) + \mathcal{F}_0$, we obtain

$$\boldsymbol{h}_{20}(0) = -g_{20}\boldsymbol{q}(0) - \bar{g}_{02}\overline{\boldsymbol{q}}(0) - \begin{bmatrix} 2\kappa\left(\frac{a}{C\tau}e^{-i\omega_0\tau} + \frac{\beta}{c\tau^2}q_{02}\right)\\ 0\end{bmatrix},$$

$$\boldsymbol{h}_{11}(0) = -g_{11}q(0) - \bar{g}_{11}\overline{\boldsymbol{q}}(0) - \begin{bmatrix} \frac{a\kappa}{C\tau}\left(e^{i\omega_0\tau} + e^{-i\omega_0\tau}\right) + \frac{\beta\kappa}{C\tau^2}\left(\overline{q}_{02} + q_{02}\right)\\ 0\end{bmatrix}.$$

On further simplifying the above equations, we get

$$\boldsymbol{h}_{20}(0) = -\frac{2i\omega_0}{C}\left(\overline{\Omega}\boldsymbol{q}_0 + \Omega\overline{\boldsymbol{q}}_0 - \begin{bmatrix}1\\0\end{bmatrix}\right), \tag{66}$$

$$\boldsymbol{h}_{11}(0) = 0. \tag{67}$$

From (46), (58), (66) and (67), we get

$$\begin{bmatrix} 2i\omega_0 w_{201}(0) + \frac{\kappa a}{\tau} w_{201}(-\tau) + \frac{\kappa\beta}{\tau^2} w_{202}(0) \\ 2i\omega_0 w_{202}(0) - \kappa w_{201}(-\tau) \end{bmatrix} = -\frac{2i\omega_0}{C}\left(\overline{\Omega}\boldsymbol{q}_0 + \Omega\overline{\boldsymbol{q}}_0 - \begin{bmatrix} 1 \\ 0 \end{bmatrix}\right), \tag{68}$$

$$\begin{bmatrix} -\frac{\kappa a}{\tau} w_{111}(-\tau) - \frac{\kappa\beta}{\tau^2} w_{112}(0) \\ \kappa w_{111}(-\tau) \end{bmatrix} = 0. \tag{69}$$

Substituting the expression for $w_{ijk}(x), x \in [-\tau, 0]$ (from (64) and (65)) in the equations (68) and (69), and solving for e_1, e_2, f_1 and f_2, we get

$$\boldsymbol{e} \equiv \begin{bmatrix} e_1 \\ e_2 \end{bmatrix} = \frac{2\tau^2}{CA_1} \begin{bmatrix} 2 \\ i\omega_0 q_{02}^2 \end{bmatrix}, \qquad \boldsymbol{f} \equiv \begin{bmatrix} f_1 \\ f_2 \end{bmatrix} = 0, \tag{70}$$

where

$$A_1 = 4\tau^2 + \kappa q_{02}^2 \left(\beta + 2ia\omega_0\tau\right).$$

Using (64), (65) and (70), we can find the solutions for $\boldsymbol{w}_{11}(0)$, $\boldsymbol{w}_{11}(-\tau)$, $\boldsymbol{w}_{20}(0)$ and $\boldsymbol{w}_{20}(-\tau)$. Using these terms, we evaluate the expression for g_{21} as

$$g_{21} = \frac{2i\overline{\Omega}\omega_0}{C^2}\left(\frac{2\Omega}{3} - \frac{A_2}{A_1}\right), \tag{71}$$

where

$$A_2 = 2\tau^2 + \kappa q_{02}^2 \left(\beta + 2ia\omega_0\tau\right).$$

Finally, we derived expressions for all the quantities required to compute the type of Hopf bifurcation and the stability of the bifurcating limit cycles. Now, we can proceed with the analysis by finding out the values of μ_2 and β_2 [11]

$$\mu_2 = \frac{-\mathbf{Re}\Big(c_1(0)\Big)}{\alpha'(0)}, \qquad \beta_2 = 2\mathbf{Re}\Big(c_1(0)\Big), \tag{72}$$

where

$$c_1(0) = \frac{i}{2\omega_0}\left(g_{20}g_{11} - 2|g_{11}|^2 - \frac{1}{3}|g_{02}|^2\right) + \frac{g_{21}}{2}, \tag{73}$$

$$\alpha'(0) = \mathbf{Re}\left(d\lambda/d\kappa\right)_{\kappa=\kappa_c}. \tag{74}$$

We now state the definitions that will enable us to investigate the nature of the Hopf bifurcation.

- The Hopf bifurcation is *super-critical* if $\mu_2 > 0$, and is *sub-critical* if $\mu_2 < 0$.

- The periodic oscillations are *asymptotically orbitally stable* if $\beta_2 < 0$ and unstable if $\beta_2 > 0$.

Substituting the expressions for the coefficients g_{20}, g_{11}, g_{02} and g_{21} in (73), we obtain

$$\begin{aligned} c_1(0) &= \frac{-i\overline{\Omega}\omega_0 A_2}{C^2 A_1}, \\ &= \frac{-i\omega_0(\beta + ia\omega_0\tau)}{C^2\big((1+i\omega_0\tau)(\beta+ia\omega_0\tau)+\beta\big)} \cdot \frac{2\kappa(\beta+ia\omega_0\tau)^2 - \omega_0^2\tau^2(\beta+2ia\omega_0\tau)}{4\kappa(\beta+ia\omega_0\tau)^2 - \omega_0^2\tau^2(\beta+2ia\omega_0\tau)}. \end{aligned} \tag{75}$$

We substitute the expressions for Ω, a and β in terms of $\omega_0\tau$ from (49) and (52) to get

$$c_1(0) = -\frac{i\omega_0}{C^2} \cdot \frac{4e^{3i\omega_0\tau} - 3e^{2i\omega_0\tau} + 1}{\big((3+2i\omega_0\tau)e^{i\omega_0\tau} + e^{-i\omega_0\tau}\big)\big(8e^{2i\omega_0\tau} - 3e^{i\omega_0\tau} + e^{-i\omega_0\tau}\big)}.$$

Let $\Theta = \omega_0\tau$, and taking the real part of the above expression, we have

$$\begin{aligned} \mathbf{Re}\big(c_1(0)\big) = &\frac{2\Theta}{C^2\tau\left(\Big(8\cos(3\Theta) - 3\cos(2\Theta) + 1\Big)^2 + \Big(8\sin(3\Theta) - 3\sin(2\Theta)\Big)^2\right)} \\ &\times \frac{1}{\big(3+\cos(2\Theta)\big)^2 + \big(2\Theta - \sin(2\Theta)\big)^2} \times \Big(4\sin(5\Theta) - 3\sin(4\Theta) \\ &- 24\sin(3\Theta) + 42\sin(2\Theta) + 4\sin(\Theta) - 12\Theta\big(2\cos(3\Theta) - \cos(2\Theta) \\ &- 6\cos(\Theta) + 7\big)\Big). \end{aligned}$$

Next, we compute the value of $\alpha^{'}(0)$. Differentiating the characteristic equation (7) with respect to κ, we get

$$\begin{aligned} \alpha'(0) &= \mathbf{Re}\left(\frac{d\lambda}{d\kappa}\right)\Bigg|_{\kappa=\kappa_c} \\ &= \frac{\Theta}{\kappa\tau} \cdot \frac{4\Theta\Big(1+\sin^2(\Theta)\Big)}{\Big(3+\cos(2\Theta)\Big)^2 + \Big(2\Theta - \sin(2\Theta)\Big)^2} > 0. \end{aligned}$$

Therefore, if $\mathbf{Re}\big(c_1(0)\big) > 0$, then $\mu_2 < 0$ (sub-critical), and $\beta_2 > 0$ (unstable limit cycles). Similarly, if $\mathbf{Re}\big(c_1(0)\big) < 0$, then $\mu_2 > 0$ and $\beta_2 < 0$, which implies that the Hopf bifurcation is super-critical, and the emerging limit cycles are orbitally asymptotically stable. In Figure 10, we plot the variation of μ_2 and β_2 as Θ is varied.
We draw the following inferences from the results of Hopf bifurcation analysis.

Remarks:

- The nature of Hopf bifurcation and the stability of limit cycles explicitly depend on Θ, where

$$\Theta = \kappa\sqrt{\frac{a^2 + \sqrt{a^4 + 4\beta^2}}{2}}.$$

- Link capacity (C) and round-trip time (τ) do not affect the sign of $\mathbf{Re}\left(c_1(0)\right)$. Hence, the type of Hopf bifurcation is independent of these system parameters.
- From Figure 10, we can note that for small values of Θ, we have $\mu_2 < 0$ and $\beta_2 > 0$, and hence the bifurcation is sub-critical and the limit cycles are unstable. Also, note that the criticality of the bifurcation changes from sub-critical to super-critical at $\Theta_h = 1.1297$. Therefore, for $\Theta > \Theta_h$, the bifurcating limit cycles are asymptotically orbitally stable.

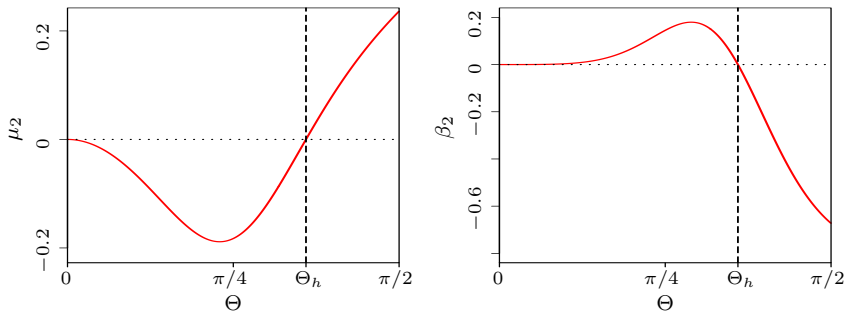

Figure 10: Variation in μ_2 and β_2 as $\Theta = \kappa\sqrt{\left(a^2 + \sqrt{a^4 + 4\beta^2}\right)/2}$ is varied. Observe that μ_2 and β_2 changes the sign at $\Theta = \Theta_h = 1.1297$. Thus, the system undergoes a sub-critical Hopf bifurcation ($\mu_2 < 0$) and the emerging limit cycles are unstable ($\beta_2 > 0$) for $\Theta < \Theta_h$. Whereas, for $\Theta > \Theta_h$, the Hopf bifurcation is super-critical and the limit cycles are asymptotically, orbitally stable.

To validate the analysis, we now perform some numerical computations for the RCP model with queue feedback. The network parameters C and τ are set to 1. We consider the following two cases.

(i) $a = 0.75$ *(sub-critical)*: Let us consider $\beta = 0.518$ that satisfies the Hopf condition at $\kappa = 1$. For these parameter values, we obtain $\mu_2 = -0.1263$ and $\mathcal{B}_2 = 0.1775$. Therefore, as per the above analytical characterization, the bifurcation is sub-critical Hopf and leads to unstable limit cycles. We use DDE-Biftool [7, 8] to plot the bifurcation diagram, see Figure 11(a). As expected from the analysis, Figure 11(a) shows that the system undergoes a sub-critical Hopf bifurcation. To illustrate the occurrence of a sub-critical Hopf, we present

some numerical simulations (using XPPAUT) in Figure 12. Considering the initial condition $R_0 = 1.03$ and $\kappa = 0.95$, the system converges to the stable equilibrium $R^* = 1$ (see Figure 12(a)). Whereas, after the bifurcation, i.e., for $\kappa > \kappa_c$, the previously stable fixed point at 1 becomes unstable and also the solution would eventually jump to infinity as shown in Figure 12(b).

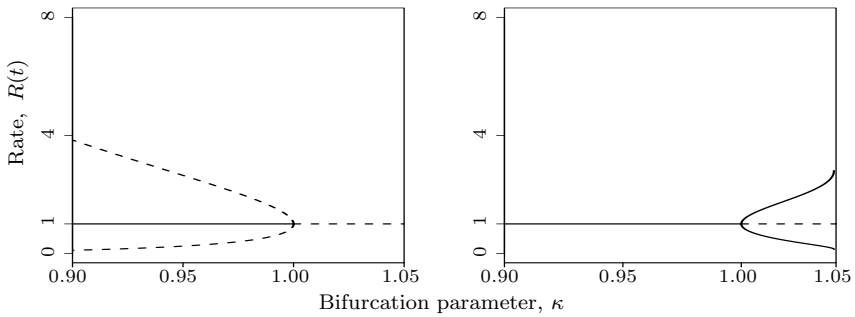

(a) $a = 0.75,\ \beta = 0.518$ (b) $a = 1.25,\ \beta = 0.454$

Figure 11: *Bifurcation diagram* for RCP model with queue size feedback. The solid line denotes an attractor and the dashed line a repeller. Observe that in case (a), the system undergoes a local *sub-critical* Hopf, while in case (b), the system undergoes a local *super-critical* Hopf bifurcation. The parameters a and β are chosen so that the system is at the Hopf condition for $\kappa = 1$. The other parameter values are $C = 1$ and $\tau = 1$.

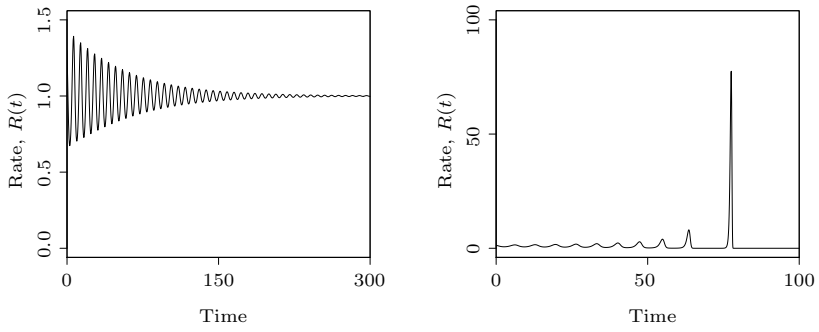

(a) $\kappa = 0.95$ (b) $\kappa = 1.05$

Figure 12: Numerical simulations highlighting that the system undergoes a sub-critical Hopf for the parameter values $a = 0.75$, $\beta = 0.518$, $C = 1$ and $\tau = 1$.

(ii) $a = 1.25$ *(super-critical)*: In this case, for the system to be at the Hopf condition with $\kappa = 1$, we take $\beta = 0.454$. Using these values, we calculate $\mu_2 = 0.1054$ and $\mathcal{B}_2 = -0.3068$. implying that the local Hopf bifurcation is super-critical and the emerging limit cycles are asymptotically orbitally stable.

The bifurcation diagram in Figure 11(b) shows the emergence of stable limit cycles, which corroborates the analysis. The numerical simulation shown in Figure 13(a) illustrates that the system is locally stable for $\kappa < 1$. But, after the occurrence of bifurcation, the system converges to a stable limit cycle (Figure 13(b)).

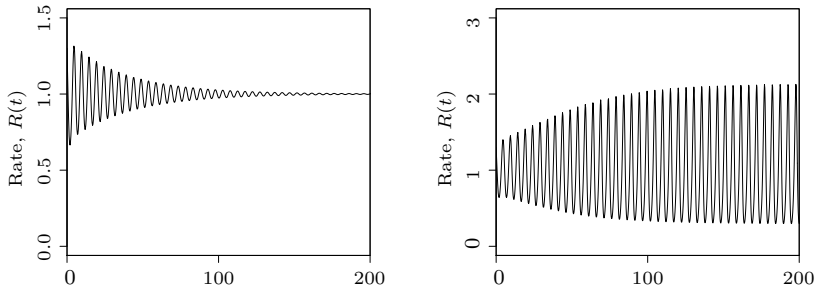

(a) $\kappa = 0.95$ (b) $\kappa = 1.05$

Figure 13: Numerical simulations illustrating the occurrence of a super-critical Hopf for $a = 1.25$, $\beta = 0.454$, $C = 1$ and $\tau = 1$.

Now, we present some packet-level simulations to illustrate that the RCP with queue feedback can undergo either super-critical or sub-critical Hopf depending on the parameter values. For this simulation, we consider $C = 1$ packet per unit time, number of flows = 100 and $\tau = 200$ time units. Simulation traces in Figure 14 (a) and Figure 14 (b) show the queue size and rate for the parameter values $a = 0.8$, $\beta = 0.55$ and $a = 1.3$, $\beta = 0.4$, respectively. For $a = 0.8$ and $\beta = 0.55$, we get $\Theta = 0.9 < \Theta_h$, and hence the type of Hopf is expected to be sub-critical. Indeed, this is confirmed in the simulation traces in Figure 14 (a) which shows the emergence of large amplitude limit cycles. However, it does not lead to blow-up due to some constraints of simulators. For the parameter values $a = 1.3$ and $\beta = 0.4$, the system exhibits a super-critical Hopf which results in small amplitude stable limit cycles (see Figure 14 (b)). This is as expected, since the values $a = 1.3$ and $\beta = 0.4$ yield $\Theta = 1.35 > \Theta_h$.

5.2. Without queue feedback

In [34], it has been shown that the equation (17) undergoes a local Hopf bifurcation at $\kappa = \kappa_c$, where $\kappa_c a = \pi/2$. If the Hopf condition is just violated, the system would lose local stability via a super-critical Hopf bifurcation and the amplitude of the bifurcating limit cycles will be proportional to

$$R^* \sqrt{\frac{20\pi(\kappa - \kappa_c)}{3\pi - 2}}. \tag{76}$$

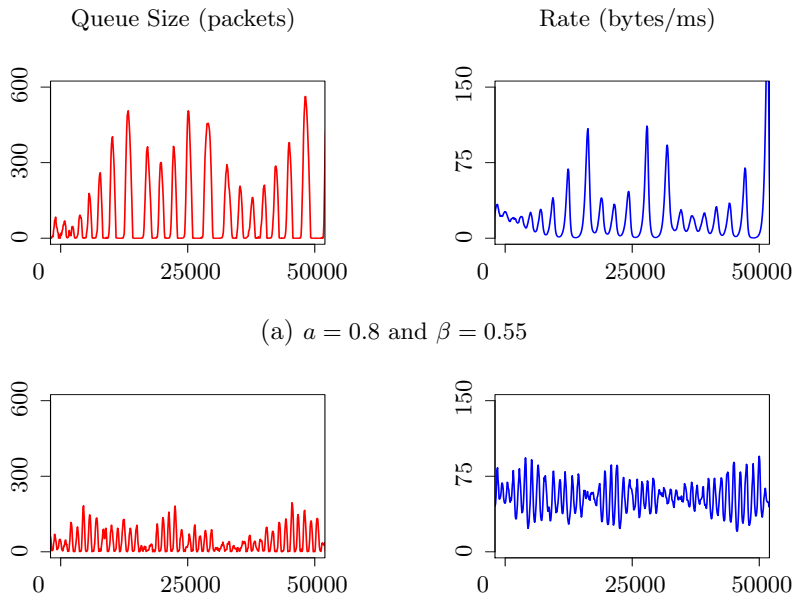

(a) $a = 0.8$ and $\beta = 0.55$

(b) $a = 1.3$ and $\beta = 0.4$

Figure 14: Simulation traces highlighting that the system which includes queue feedback exhibit sub-critical Hopf and super-critical Hopf for the parameter choices $a = 0.8$, $\beta = 0.55$ and $a = 1.3$, $\beta = 0.4$, respectively. We consider the number of flows as 100, and each with round-trip time of 200 time units.

Here R^* denotes the equilibrium of (17). It is also highlighted in [34] that equation (17) cannot undergo a sub-critical Hopf bifurcation.

Discussion: It is rather striking to find the possibility of a sub-critical Hopf bifurcation in RCP. A sub-critical Hopf would lead either to the emergence of unstable limit cycles, or to the emergence of limit cycles with a very large amplitude. Either of these outcomes is detrimental to system performance and is undesirable in engineering applications. Therefore, in the design of congestion control algorithms in which there is a possibility of violation of the conditions for local stability, an important design objective is not only to make sure that the system is stable, but also to ensure any loss of system stability produces stable limit cycles with small amplitude. Thus, the results of Hopf bifurcation analysis favors the design choice which uses only rate mismatch feedback.

6. Condition for non-oscillatory convergence

Non-oscillatory convergence is a desirable characteristic in the design of dynamical systems. In this section, we derive a necessary and sufficient condition to ensure non-oscillatory convergence of RCP which uses only rate mismatch feedback.

For the system to be non-oscillatory, the eigenvalues should be negative real numbers. Recall that the characteristic equation of the RCP without queue size feedback is

$$\lambda + \left(\frac{a}{\tau}\right) e^{-\lambda\tau} = 0. \tag{77}$$

Substituting $\lambda = -\sigma + j\omega$ in (77) gives

$$\sigma = \frac{a}{\tau} e^{\sigma\tau} \cos(\omega\tau), \tag{78}$$

$$\omega = \frac{a}{\tau} e^{\sigma\tau} \sin(\omega\tau). \tag{79}$$

Solving the equations (78) and (79) yields

$$\sigma\tau = \frac{\omega\tau}{\tan(\omega\tau)}. \tag{80}$$

The right hand side of (80) is a decreasing function of ω, and has a maximum value of 1 at $\omega = 0$. For the uniqueness of the solution, we require $\sigma\tau \geq 1$. Now, (79) can be rewritten as

$$ae^{\sigma\tau} \frac{\sin(\omega\tau)}{\omega\tau} = 1. \tag{81}$$

Taking the limit $\omega \to 0$ gives

$$\lim_{\omega\to 0} \; ae^{\sigma\tau} \frac{\sin(\omega\tau)}{\omega\tau} = ae^{\sigma\tau}, \tag{82}$$

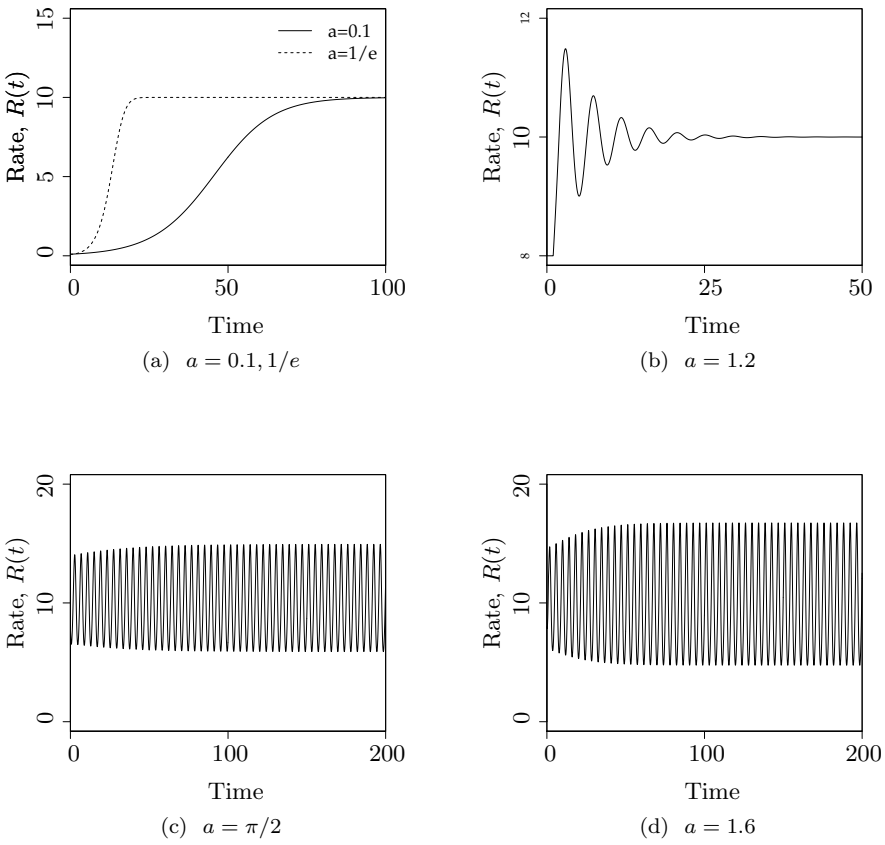

(a) $a = 0.1, 1/e$ (b) $a = 1.2$

(c) $a = \pi/2$ (d) $a = 1.6$

Figure 15: Numerical simulations showing the behavior of the system for various values of the protocol parameter a. The parameter values used are $C = 10$ and $\tau = 1$.

and hence $ae^{\sigma\tau} = 1$. Since $\sigma\tau \geq 1$, then $a \leq (1/e)$. Thus, the necessary and sufficient condition for non-oscillatory convergence of RCP without queue size feedback is

$$a \leq \frac{1}{e}. \tag{83}$$

After analyzing the condition for non-oscillatory convergence, and the rate of convergence, it can be deduced that the rate of convergence is maximum at the boundary of non-oscillatory regime, i.e., $a = 1/e$. Thus, the analytical results reveals that the optimal value of the protocol parameter a is $1/e$. The system becomes oscillatory when $a > 1/e$, and hence the rate of convergence decreases. At $a = \pi/2$, the convergence rate is zero and the reason behind is that the system transits into unstable regime via a Hopf bifurcation at $a = \pi/2$.

To validate the theoretical results of non-oscillatory convergence, numerical

Table 1: Effect of the value of protocol parameter on the system behavior. At $a = 1/e$, the system reaches equilibrium quickly without any oscillations.

Parameter range	System behavior
$a \in (0, 1/e]$	stable and non-oscillatory
$a \in (1/e, \pi/2)$	stable and oscillatory
$a \geq \pi/2$	unstable

simulations obtained using XPPAUT are shown in Figure 15. As can be observed in Figure 15 (a), for $a = 0.1$ ($< 1/e$), the system shows over-damped behavior, i.e., reaches equilibrium without oscillating. At $a = 1/e$, the system reaches equilibrium as quickly as possible without any oscillations. For $a \in (1/e, \pi/2)$, the system behaves in an under-damped manner, i.e., existence of convergent oscillations (see Figure 15 (b)). As shown in Figure 15 (c) and Figure 15 (d), the system loses stability at $a = \pi/2$, and the amplitude of the undamped oscillations increases as a increases beyond $\pi/2$.

The dependence of system behavior on the protocol parameter value is summarized in (1).

7. Conclusions

The design of explicit congestion control protocols is an important research topic among the networking research community. The Rate Control Protocol (RCP) is a well-known explicit feedback algorithm that utilizes router feedback based on rate mismatch and queue size. However, it is currently an open question if the protocol definition should include two forms of feedback; i.e., both rate mismatch and queue feedback. In this paper, we developed a better understanding of this design choice, using tools from control and bifurcation theory. In particular, we considered stability, convergence and the impact of the loss of local stability on system dynamics.

Local stability analysis was conducted both in the presence and absence of queue size feedback and established necessary and sufficient conditions to ensure local stability. This enabled us to determine bounds on the protocol parameters to guarantee the local stability of the system. The rate of convergence analysis highlighted that the queue term should be excluded from the protocol to improve the convergence rate. Also, a necessary and sufficient condition that guarantees non-oscillatory convergence was derived for RCP where the queue size term is absent. This condition enabled us to suggest an optimal value of the protocol parameter.

Further, we also showed that in the presence of queue feedback, the system readily loses its stability via a Hopf bifurcation, as the bifurcation parameter varies. For our analyses, a dimensionless exogenous parameter was used as the bifurcation parameter. The phenomenon of Hopf bifurcation would result in the onset of limit cycles which make it harder to control the queue size. We analyzed the Hopf bifurcation properties by applying Poincaré normal forms and

the center manifold theorem. We showed that, for some parameter values, the presence of queue feedback in the RCP model leads to a sub-critical Hopf bifurcation and the emergence of unstable limit cycles. But, in the absence of queue feedback, the Hopf bifurcation is super-critical, and the bifurcating periodic solutions are asymptotically orbitally stable. In essence, all our insights revealed that the performance of the RCP could be improved by removing the queue size term from the protocol definition. Thus, based on our current analysis, we suggest it is preferable to go with the design choice that uses only rate mismatch feedback. However, this is a critical design consideration, and additional analysis and experimental results would be needed to arrive at a comprehensive understanding.

A natural extension of this study would be to validate the analytical insights through hardware experiments. In the real network environment, flows arrive and depart dynamically, and also can have heterogeneous round-trip times. Thus, future research should also include an in-depth analysis of the impact of queue feedback on the performance of the system with multiple time delays, and for a variety of flow arrival and departure patterns.

References

References

[1] G. Allon and A. Bassamboo, "The impact of delaying the delay announcements", *Operation Research*, vol. 59, pp. 1198–1210, 2011.

[2] H. Balakrishnan, N. Dukkipati, N. McKeown and C.J. Tomlin, "Stability analysis of explicit congestion control protocols", *IEEE Communications Letters*, vol. 11, pp. 823–825, 2007.

[3] L. Baretto, "XCP-Winf and RCP-Winf: Improving Explicit Wireless Congestion Control", *Journal of Computer Networks and Communications*, pp. 1–18, 2015.

[4] F. Brauer, "Decay rates for solutions of a class of differential-difference equations", *SIAM Journal on Mathematical Analysis*, vol. 10, pp. 783–788, 1979.

[5] B. Dubey, A. Kumar and A.P. Maiti, "Global stability and Hopf-bifurcation of prey-predator system with two discrete delays including habitat complexity and prey refuge", *Communications in Nonlinear Science and Numerical Simulation,* vol. 67, pp. 528–554, 2019.

[6] N. Dukkipati, N. McKeown and A.G. Fraser, "RCP-AC: Congestion control to make flows complete quickly in any environment", in *Proceedings of IEEE International Conference on Computer Communications*, 2006.

[7] K. Engelborghs, T. Luzyanina and D. Roose, "Numerical bifurcation analysis of delay differential equations using DDE-Biftool", *ACM Transactions on Mathematical Software*, vol. 28, pp. 1–21, 2002.

[8] K. Engelborghs, T. Luzyanina and G. Samaey, "DDE-Biftool v. 2.00: a Matlab package for bifurcation analysis of delay differential equations", *Technical Report TW-330*, Department of Computer Science, K.U. Leuven, Leuven, Belgium, 2001.

[9] B. Ermentrout, *Simulating, Analyzing, and Animating Dynamical Systems: A Guide to XPPAUT for Researchers and Students*. SIAM Publications, 2002.

[10] F.S. Gentile, J.L. Moiola and E.E. Paolini, "Nonlinear dynamics of Internet congestion control: a frequency-domain approach", *Communications in Nonlinear Science and Numerical Simulation*, vol. 19, no. 4, pp. 1113–1127, 2014.

[11] B.D. Hassard, N.D. Kazarinoff and Y.H. Wan, *Theory and Applications of Hopf Bifurcation*. Cambridge University Press, 1981.

[12] N.D. Hayes, "Roots of the transcendental equation associated with a certain differential-difference equation", *Journal of the London Mathematical Society,* vol. 25, pp. 226-232, 1950.

[13] L. He and H. Zhou, "Robust Lyapunov-Krasovskii based design for explicit control protocol against heterogeneous delays", *Telecommunication Systems*, vol. 63, no. 3, pp. 377–392, 2017.

[14] C. Huang, J. Cao, M. Xiao, A. Alsaedi and T. Hayat, "Effects of time delays on stability and Hopf bifurcation in a fractional ring-structured network with arbitrary neurons", *Communications in Nonlinear Science and Numerical Simulation*, vol. 57, pp. 1–13, 2018

[15] D. Katabi, M. Handley and C. Rohrs, "Congestion control for high bandwidth-delay product networks", *ACM SIGCOMM Computer Communication Review,* vol. 32, no. 4, pp. 89–102, 2002.

[16] F. Kelly and G. Raina, *Explicit Congestion Control: charging, fairness and admission management, Next-Generation Internet: Architectures and Protocols*, pp. 257-274, Cambridge University Press, 2011.

[17] F. Kelly, G. Raina and T. Voice, "Stability and fairness of explicit congestion control with small buffers", *ACM SIGCOMM Computer Communication Review,* vol. 38, no. 3, pp. 51–62, 2008.

[18] L. Khoshnevisan, X. Liu and F.R. Salmasi, "Stability and Hopf bifurcation analysis of a TCP/RAQM network with ISMC procedure", *Chaos, Solitons & Fractals*, vol. 118, pp. 255–273, 2019.

[19] A. Lakshmikantha, R. Srikant, N. Dukkipati, N. McKeown and C. Beck, "Buffer sizing results for RCP congestion control under connection arrivals and departures", *ACM Computer Communication Review*, vol. 39, pp. 5–15, 2008.

[20] K. Lei, C. Hou, L. Li and K. Xu, "A RCP-based congestion control protocol in Named Data Networking", in *Proceedings of International Conference on Cyber-Enabled Distributed Computing and Knowledge Discovery*, 2015

[21] F. Liu, O.H. Wang and Z.H. Guan, "Hopf bifurcation control in the XCP for the Internet congestion control system", *Nonlinear Analysis: Real World Applications,* vol. 13, no. 3, pp. 1466–1479, 2008.

[22] F. Liu, Z.H. Guan and O.H. Wang, "Stability and Hopf bifurcation analysis in a TCP fluid model", *Nonlinear Analysis: Real World Applications*, vol. 12, no. 1, pp. 353-363, 2011.

[23] M. Mahdian, S. Arianfar, J. Gibson and D. Oran, "MIRCC: Multipath-aware ICN rate-based congestion control", in *Proceedings of ACM Conference on Information-Centric Networking*, 2016.

[24] S. Novitzky, J. Pender, R.H. Rand and E. Wesson, "Non-linear dynamics in queueing theory: Determining size of oscillations in queues with delayed information", *SIAM Journal on Applied Dynamical Systems*, vol. 18, pp. 279–311, 2019.

[25] J. Pender, R.H. Rand and E. Wesson, "An analysis of queues with delayed information and time-varying arrival rates", *Nonlinear Dynamics,* vol. 91, pp. 2411–2427, 2018.

[26] L. Pei and L. Yang, "Prediction of period-1 oscillations of the state-dependent delayed compound TCP model with PIE queue management policy via HDHBM", *Communications in Nonlinear Science and Numerical Simulation*, vol. 67, pp. 26–36, 2019.

[27] L. Pei and Y. Wu,"Hopf bifurcation of the wireless network congestion model with state-dependent round trip delay", *International Journal of Bifurcation and Chaos*, vol. 28, no. 9, 2018.

[28] Y. Ren, J. Li, S. Shi, L. Li and G. Wang, "An explicit congestion control algorithm for named data networking", in *Proceedings of IEEE International Conference on Computer Communications*, 2016.

[29] V. Sharma, "Queues with service rate controlled by a delayed feedback", *Queueing Systems*, vol. 39, pp. 303–315, 2001.

[30] N.K. Sharma, A. Kaufmann, T.E. Anderson, A. Krishnamurthy, J. Nelson and S.Peter, "Evaluating the power of flexible packet processing for network resource allocation", in *Proceedings of USENIX Symposium on Networked Systems Design and Implementation*, 2017.

[31] R. Srikant, *The Mathematics of Internet Congestion Control*, Springer Science and Business Media, 2012.

[32] S.H. Strogatz, *Nonlinear dynamics and chaos: with applications to physics, biology, chemistry, and engineering,* CRC Press, 2018.

[33] Y.D. Sun, Z.Z. Ji and H. Wang, "Towards performance evaluation of Rate Control Protocol in satellite networks", *International Journal of Electrical and Computer Sciences*, vol. 12, pp. 37–41, 2012.

[34] T. Voice and G. Raina, "Stability analysis of a max-min fair Rate Control Protocol (RCP) in a small buffer regime", *IEEE Transactions on Automatic Control,* vol. 54, no. 8, pp. 1908–1913, 2009.

[35] B. Wydrowski and M. Zukerman, "MaxNet: A congestion control architecture for max-min fairness", *IEEE Communications Letters*, vol. 6, no. 11, pp. 512–514, 2002.

[36] L. Zhang, D. Estrin, J. Burke, V. Jacobson, J.D. Thornton, D.K. Smetters, B. Zhang, G. Tsudik, D. Massey and C. Papadopoulos, "Named Data Networking (NDN) project," PARC, Technical Report NDN-0001, Oct. 2010.

[37] Y. Zhang, D. Leonard and D. Loguinov, "JetMax: Scalable max-min congestion control for high-speed heterogeneous networks", *Computer Networks*, vol. 52, no. 6, pp. 1193–1219, 2008.

[38] S. Zhang, J. Xu and K.W. Chung, "On the stability and multi-stability of a TCP/RED congestion control model with state-dependent delay and discontinuous marking function", *Communications in Nonlinear Science and Numerical Simulation*, vol. 22, pp. 269–284, 2015.

[39] S. Zhong, Y. Liu, J. Li and K.Lei, "A rate-based multipath-aware congestion control mechanism in named data networking", in *Proceedings of IEEE International Symposium on Ubiquitous Computing and Communications*, 2017.